Life Sciences 233 (2019) 116730

Contents lists available at ScienceDirect

Life Sciences

journal homepage: www.elsevier.com/locate/lifescie

Dihydroartemisinin suppresses glycolysis of LNCaP cells by inhibiting PI3K/AKT pathway and downregulating HIF-1α expression

Wenhe Zhu[1], Yawei Li[1], Donghai Zhao, Huilin Li, Wei Zhang, Junjie Xu, Jiancheng Hou, Xianmin Feng*, Huiyan Wang**

Jilin Medical University, Ji Lin, China

ARTICLE INFO

Keywords:
Dihydroartemisinin
Prostate cancer
Glycolysis
Akt/mTOR
HIF-1 α

ABSTRACT

Aims: Dihydroartemisinin (DHA) exhibits potential anticancer activity. However, the biological functions of DHA in prostate cancer remain largely unexplored. In this study, we aim to investigate the anti-proliferative effect and glycolysis regulation of DHA on prostate cancer cell LNCaP.

Main methods: Cell proliferative activity and apoptosis inducing were detected. The gene expression was detected by mRNA microarray and results were analyzed by GO and KEGG pathway database. Expressions of glycolysis key enzymes and PI3K/AKT/HIF-1α were detected by Western blot.

Key findings: Results indicated that DHA could inhibit the LNCaP cell proliferation considerably and induce cell apoptosis. mRNA microarray showed 1293 genes were upregulated and 2322 genes were downregulated. GO and KEGG enrichment analysis suggested that glycolysis pathway was correlated with DHA inhibited the proliferation on the LNCaP cell. Western blot results showed that DHA can decrease GLUT1 and regulatory enzymes of glycolytic pathway expression probably by suppressing the activity of the intracellular Akt/mTOR and HIF-1 α.

Significance: Experimental validation results indicate that DHA treatment can inhibit the LNCaP cell proliferation and induce apoptosis, which may be related to glycolysis inhibition.

1. Introduction

Prostate cancer is one of the most common malignant tumors that affect men around the world. According to data from the World Health Organization, prostate cancer causes approximately 1.1 million newly diagnosed cases and 307,000 deaths annually worldwide in 2017 [1,2]. Localized prostate cancer at the early stage can be treated by radical prostatectomy with a good prognosis [3]. Advanced prostate cancer patients are mostly treated by androgen-deprivation therapy, which fails eventually, leading to the development of incurable and lethal castration-resistant prostate cancer [4–6]. Therefore, the discovery of new therapeutic agents and approaches for prostate cancer is of paramount importance.

Traditional Chinese medicine and related natural active ingredients provide rich resources for the development of modern medicine [7]. For instance, artemisinin (ART), a sesquiterpene lactone that bears a peroxide grouping, was isolated by Chinese pharmacist Youyou Tu and colleagues from the leaf of the herb *Artemisia annua* L., which has been developed as an anti-malarial drug and used worldwide [8,9]. Unexpectedly, studies have found that dihydroartemisinin (DHA), an ART-derived antimalarial drug approved by the United States Food and Drug Administration, which displayed effective anti-tumor effect *in vitro* and *in vivo* [10]. Studies have shown that DHA can inhibit the proliferation of leukemia, brain glioma, and cancers of the liver, breast, lungs, cervix, pancreas, and ovaries [11,12]. The possible mechanism may be related to inhibiting the proliferation and inducing apoptosis of tumor cells, arresting the cell cycle, and inhibiting tumor cell invasion and metastasis [13]. In the current study, the ART-type drugs are the pathway to clinical therapy in some types of tumors [14]. However, limited experimental research has examined the potential of DHA in treating prostate cancer. The exact molecular mechanisms of DHA anticancer effects on prostate have yet to be fully investigated.

Metabolic change is a hallmark of tumor, which has recently attracted much attention. One of the main metabolic characteristics of tumor cells is the high level of glycolysis even in the presence of oxygen; this condition is known as aerobic glycolysis or Warburg effect

* Corresponding author.
** Correspondence to: H. Wang, Ji Lin Medical University, Ji Lin 132013, China.
E-mail address: jlmpcwhy@163.com (H. Wang).
[1] Equal contribution.

https://doi.org/10.1016/j.lfs.2019.116730
Received 6 July 2019; Received in revised form 26 July 2019; Accepted 3 August 2019
Available online 04 August 2019
0024-3205/

[15,16]. Glycolysis supplies abundant energy to sustain the rapid tumor growth. Moreover, products of glycolysis, such as lactate, provide a suitable microenvironment to promote tumor metastasis [17,18]. Thus, inhibiting tumor aerobic glycolysis to block energy supply has been certified as an effective strategy to overcome difficulties in cancer treatment, and the validity has been proven in relevant pre-clinical studies. To date, few studies on prostate cancer energy metabolism have been published [19,20]. By understanding the relationship between glucose glycolysis and tumorigenesis, we propose that blocking tumor glucose glycolysis is an effective treatment strategy in exploring anti-tumor agents for prostate treatment. In the present study, we aim to explore the cell growth inhibition effect of DHA against prostate cancer and examine its mechanisms, including the alteration of metabolic phenotype and apoptosis. This study provides insights into the molecular mechanisms of DHA against cancer cells and demonstrates that DHA may be a promising new agent for prostate treatment.

2. Materials and methods

2.1. Materials, cell culture, and proliferation assay

Human prostate cancer cell line LNCaP was provided by Chinese Academy of Sciences (Shanghai, China) and preserved in the Department of Biochemistry, Jilin Medical University. Dulbecco's Modified Eagle's Medium (DMEM) and fetal bovine serum (FBS) were purchased from Thermo Fisher Scientific (USA). Dimethyl sulfoxide (DMSO, analytical grade) was obtained from Beijing Chemical Reagent Factory (Beijing, China). DHA was obtained from Sigma-Aldrich (USA). The mouse anti-human HIF-1α antibody (sc-13,515, 1:1000), mouse anti-human PFKP antibody (sc-514,824, 1:1000), and mouse anti-human LDH antibody (sc-133,123, 1:1000) were obtained from Santa Cruz Biotechnology (Santa Cruz, USA). Rabbit anti-human p-AKT antibody (ab18206, 1:1000), rabbit anti-human AKT antibody (ab8805, 1:1000), rabbit anti-human p-MTOR antibody (ab84400, 1:1000), and rabbit anti-human MTOR antibody (ab2732, 1:1000) were obtained from Abcam Inc. (Abcam, USA). Rabbit anti-human Glut1 antibody (SAB4502803, 1:1000), rabbit anti-human PKM2 antibody (SAB4200105, 1:1000), and rabbit anti-human HK2 antibody (SAB2701698, 1:1000) were purchased from Sigma-Aldrich Company (St. Louis, MO, USA).

LNCaP cells were maintained in DMEM supplemented with 10% FBS, 100 units/mL of penicillin, and 100 units/mL of streptomycin at 37 °C in a humidified atmosphere of 5% carbon dioxide (CO_2) and 95% air. The cells were sub-cultured every 3 days with 0.25% trypsin. The proliferation inhibition of DHA on tumor cells was detected by MTT assay [21]. LNCaP cells were seeded into a 96-well assay plate with a concentration of 1.0×10^5 cells/mL (200 μL per well). After 48 h incubation, the cells were treated with DHA at 0–160 μM concentration in the growth medium. Each concentration was tested five times. The cells were cultured for another 48 h. Subsequently, 20 μL MTT (5 mg/mL) was added to each well and incubated for another 4 h. Then, the supernatant was discarded and 150 μL DMSO was loaded to each well. The optical density (OD) was measured at 490 nm using a Bio-assay reader (Bio-Rad 550, USA).

2.2. Apoptosis assay

LNCaP cells were cultured on slides at a density of 5×10^4/mL in 24-well plates. After treatment with different concentrations of DHA, the medium was removed, and the cells were washed twice with PBS. Then, the cells were fixed with 4% paraformaldehyde for 10 min. Subsequently, the cells were stained by Hoechst 33258 for 5 min. Then, the apoptosis morphology was observed by a fluorescence microscope.

After treatment with different concentrations of DHA, the LNCaP cells were harvested by centrifugation at 1000*g* for 3 min and washed twice with PBS. The harvested cell pellet was re-suspended in 100 μL DMEM medium. Then, 100 μL Muse Annexin V & Dead Cell reagents were added and incubated at room temperature for 20 min. The percentages of apoptosis were detected by using a Muse Cell Analyzer (Merck-Millipore).

2.3. mRNA microarray profiling

The mRNA microarray expression profiling was performed on three biological replicates of DHA-treated or untreated groups. After DHA treatment, the total cellular RNA was isolated using TRIzol reagent (Invitrogen, CA) and quantified by NanoDrop ND-2000 (Thermo Scientific). RNA integrity was assessed using Agilent Bioanalyzer 2100 (Agilent Technologies). The samples with an RNA integrity number (RIN) > 7 were used to construct the sequencing library. The sample labeling, microarray hybridization, and washing were performed based on the manufacturer's standard protocols. Briefly, the total RNA was transcribed to double-stranded cDNA and then synthesized into cRNA and labeled with Cyanine-3-CTP. The labeled cRNAs were hybridized onto the microarray. After washing, the arrays were scanned by the Agilent Scanner G2505C (Agilent Technologies).

Feature Extraction software (version 10.7.1.1, Agilent Technologies) was used to analyze the array images to obtain raw data. GeneSpring (version 14.8, Agilent Technologies) was employed to complete the basic analysis of raw data. Differentially expressed genes (DEGs) were then identified through fold change, and *P* value was calculated with *t*-test. The threshold set for up- and down-regulated genes was a fold change ≥ 2.0 and a *P* value ≤ 0.05. Afterward, Gene Ontology (GO; http://www.geneontology.org/) and Kyoto Encyclopedia of Genes and Genomes (KEGG; http://www.genome.jp/kegg/) analyses were conducted to determine the roles of these differentially expressed mRNAs. Finally, hierarchical clustering was performed to display the distinguishable gene expression patterns among samples.

2.4. Quantitative reverse transcription polymerase chain reaction (qRT-PCR)

The expression of selected genes was characterized using total RNA extracted from AT-treated and untreated LNCap cells. Real-time RT-PCR was performed on RNA samples using gene-specific oligonucleotide primers (Table. S1), iScript One-Step RT-PCR Kit with SYBR Green, and CFX96 Touch Real-Time PCR Detection System (Bio-Rad, Hercules, CA). All values were normalized to β-actin and standardized to the control condition. Error bars represent THE standard error of the mean (SEM), and the statistical significance was assessed using Student's *t*-test. After completion of RT-PCR, the Ct values were obtained from the ABI 7500 fast v2.0.1 software. The ΔΔCt method was used to represent mRNA fold change.

2.5. Measurements of glucose uptake levels, lactate production, and ATP content

The LNCaP cells were seeded in six-well plates at a density of 1×10^4 cells/well. After treatment with DHA for 48 h, the cell culture media were collected for the detection of glucose uptake and lactate production. For the assessment of lactate production, the collected culture media were diluted to 1:50 volume by using lactate assay buffer. The amount of lactate present in the media was then estimated using the Lactate Assay Kit (Sigma, St. Louis, MO, USA) according to the manufacturer's instructions. The glucose content in the collected culture media was detected immediately following the manufacturer's instructions for the Glucose Assay Kit.

The LNCaP cells were seeded in six-well plates (1×10^5 cells/mL) and incubated with DHA for 48 h. Then, the cells were harvested and lysed ice with somatic cell ATP-releasing reagent. ATP content was detected by ATP assay kits (Genmed Scientifics, Inc., Wilmington,

Delaware, USA) according to the manufacturer's instructions. Glucose uptake, lactate production, and ATP content were all normalized by cell number.

2.6. Western blot analysis

After DHA treatment, 5×10^5 LNCaP cells were harvested and lysed in PIPA buffer to extract the total protein. The extracted total protein content was determined by Bio-Rad protein assay kit, and 50 μg protein/lane was loaded on the gel for sodium dodecyl sulfate polyacrylamide gel electrophoresis (SDS-PAGE). After SDS-PAGE, the separated proteins were transferred to nitrocellulose membranes. Nonspecific binding was blocked by incubating nitrocellulose membranes in 5% non-fat dry milk in TBS/0.1% Tween for 120 min. After blocking, the blots were incubated with primary antibodies at 4 °C overnight. Then, the appropriate secondary antibodies were added and incubated for 1 h at room temperature. Immunoreactive protein bands were detected by using enhanced chemiluminescence (ECL) reagents.

2.7. Statistical analysis

The results are presented as mean ± SEM, which are derived from three or more independent experiments. All data were analyzed by one-way ANOVA using SPSS version 13 software. $p < 0.05$ was considered significant.

3. Results

3.1. DHA inhibits proliferation of LNCaP cells

We conducted MTT assay to evaluate the cytotoxic effects of DHA on LNCaP cells and examine the proliferation of LNCaP cells upon DHA treatment. The LNCaP cells were treated with increasing doses of DHA (10, 20, 40, 80, 120, and 160 μM) for 48 h. MTT results showed that DHA could inhibit the proliferation of LNCaP in a dose-dependent manner (Fig. 1A). To investigate whether DHA inhibits the proliferation of LNCaP cells by inducing apoptosis, we examined the nuclear morphology of LNCaP cells following different concentrations of DHA treatment. We employed Hoechst 33258 staining, which is considered a potential apoptosis marker in detecting apoptotic nuclei. As shown in Fig. 1B, the cell nucleus emerged as a uniform blue chromatin with an organized structure in the control group cells. After treatment with DHA at concentrations of 20, 40, and 80 μM for 48 h, the LNCaP cells decreased in number and nuclear size and exhibited a strong fluorescent spot, pyknotic nuclei, and extensive blebbing. The presence of condensing chromatin and apoptotic bodies was observed under a fluorescence microscope, thereby indicating that the apoptosis of LNCaP cells was induced by DHA.

Similar results were obtained from staining by Muse Annexin V & Dead Cell assay. The percentage of early apoptotic cells increased with the increased dose of DHA compared with the untreated group ($p < 0.01$) (Fig. 1C and D).

3.2. mRNA microarray expression profiling data analysis

We applied mRNA microarray to explore the potential inhibition mechanism of DHA and detect the differential gene expression in LNCaP cells between DHA treatment and control groups. We selected the 40 μM dose, which is suitable for transcriptome analysis, to reveal the full mechanism of DHA action on LNCaP cells. After DHA treatment, the cells from DHA-treated (D) and untreated groups (C) were extracted to analyze the quality and integrity of each sample by using an ultraviolet spectrophotometer. First, we must ensure the quality and integrity of the total RNA purified from each sample. The ration of A260/280 is 2.0 for the samples, indicating RNA purity. The quality and integrity of the total RNA was also assessed using formaldehyde agarose gel electrophoresis. The electrophoretogram of both samples in C and D group showed distinctive bands corresponding to 28S and 18S ribosomal RNA, respectively. The results indicate that the total RNA extracted from both samples was intact and non-degraded and adequate for the subsequent gene chip experiment (Fig. 2A). Meanwhile, principal component analysis (PCA) of samples was performed on the complete dataset. The PCA results demonstrated that the samples were separated into two clusters (Fig. 2B), indicating a distinct directionality in the different groups based on similarities in gene expression. These results certified the samples available for subsequent analyses. Thereafter, the DEGs were identified. The DEGs resulting from DHA treatment were described by volcano plots. Multiple testing correction used the Benjamini–Hochberg method with a corrected $p < 0.05$ and a 2.0-fold change cutoff. By comparing the microarray expression profiling data from the control (C) and DHA (M) treatment cells, we identified 3615 DEGs, among which 1293 were upregulated, and 2322 were downregulated (Fig. 2C, Table S2).

Using the data on microarray analysis, we perform GO and KEGG analysis. According to GO classification, three domains were covered: biological processes (BP), cellular components (CC), and molecular function (MF). In the BP domain, mitotic nuclear division and high proportion of DEGs are related to mitotic nuclear division, cell division, DNA replication, G_2/M transition of mitotic cell cycle, and nucleosome assembly (Fig. 3A). In the CC domain, the enriched parts cover the nucleoplasm, cytosol, cytoplasm, nucleus, and nuclear chromatin (Fig. 3B). In the MF domain, ATP binding, protein binding, single-stranded DNA-dependent ATPase activity, ATPase activity, and protein heterodimerization activity were affected by DHA treatment (Fig. 3C). KEGG pathway enrichment analysis revealed that DHA treatment influences diverse pathways. Cell cycle, DNA replication, p53 signaling pathway, glycolysis/gluconeogenesis, metabolic pathways, pyrimidine metabolism, HIF-1 signaling pathway, and biosynthesis of amino acids were among the top 20 pathways (Fig. 3D).

From the GO and pathway enrichment results, we observed that the metabolic process was involved in the DHA inhibition of the proliferation of LNCaP cells. Specifically, the gene expressions of key enzymes in the glycolysis/gluconeogenesis were downregulated (Fig. 4). To confirm the microarray results, we conducted qPCR to analyze four genes that exhibited differential expressions upon DHA treatment. Consistent with the microarray results, AR, HK2, PFKP, and PGK1 were also downregulated upon DHA treatment by qPCR (Fig. 5).

3.3. DHA for glycolysis inhibition

Tumor cells use glucose as substrate for ATP synthesis and production of components of cellular metabolism. We detected glucose uptake in LNCaP cells after 40 μM DHA treatment for 48 h. The results indicate that glucose uptake decreased in DHA-treated LNCaP cells (Fig. 6A). The main products of glycolysis are lactic acid and ATP. The lactic acid and ATP contents were detected by relevant reagent kits to investigate whether glycolysis inhibition was involved in the proliferation inhibition of LNCaP by DHA. The results indicate that the contents of intracellular ATP and extracellular lactic acid declined in the LNCaP cells after DHA treatment compared with the control group (Fig. 6B and C).

The expressions of Glut1, HK2, PFKP, PKM2, and LDH were detected by Western blot to assess whether DHA regulates the expression of glycolytic regulator proteins in LNCaP cells. As shown in Fig. 7, the expressions of GLUT1, HK2, PFKP, PKM2, and LDH in DHA-treated LNCaP cells decreased (Fig. 7), suggesting that DHA may inhibit glycolysis by suppressing the expressions of key enzymes.

3.4. DHA decreases HIF-1α via PI3K/AKT pathway

The PI3K/Akt pathway is known to be involved in glucose metabolism. HIF-1α, which is regulated by the PI3K/Akt pathway, induces

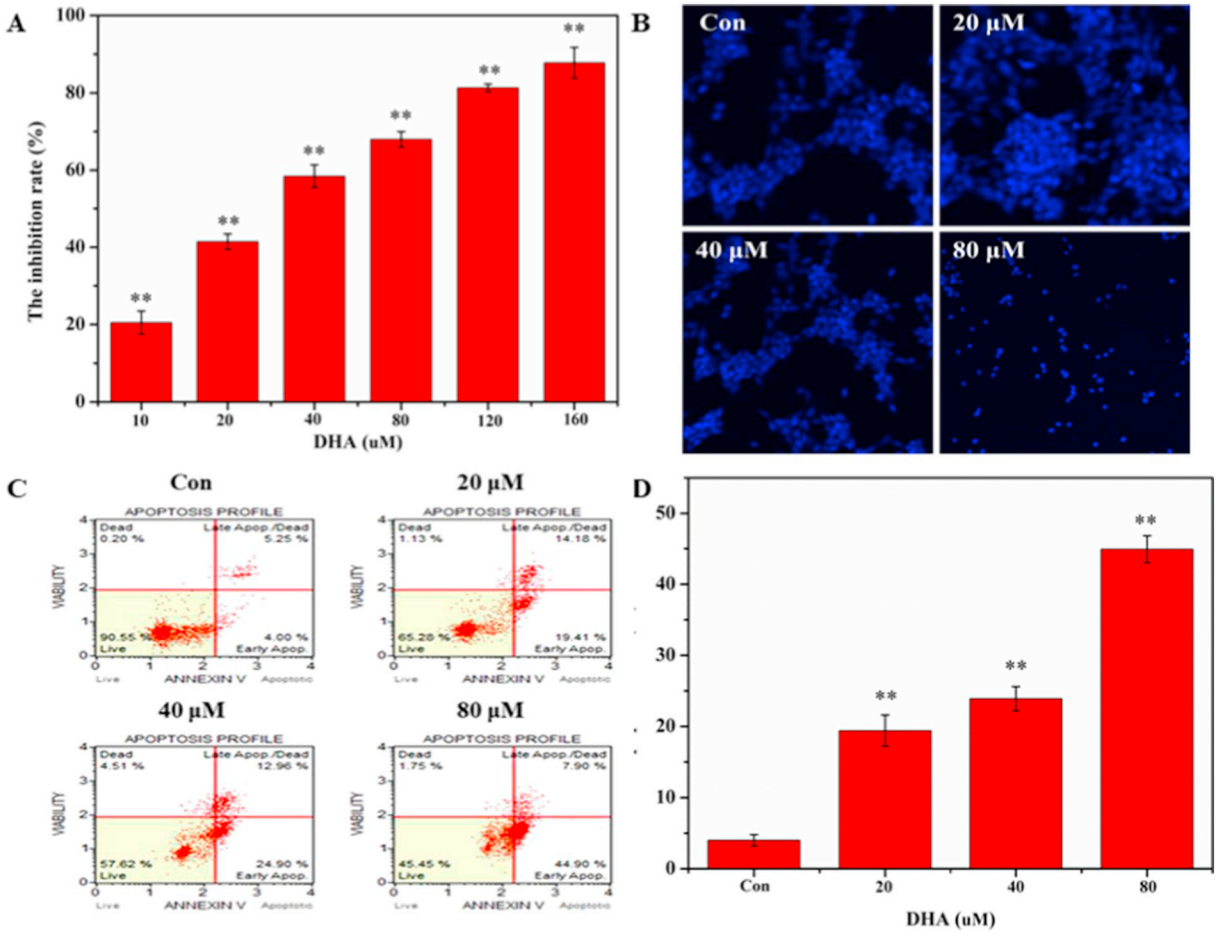

Fig. 1. DHA inhibits LNCaP cell proliferation and induces apoptosis. (A) LNCaP cells were treated with increasing concentrations of DHA for 48 h. Cell growth inhibition activity was assessed by MTT assay. (B) After treatment with DHA for 48 h, the cells were stained with Hoechst 33258, and apoptotic morphological change was detected by fluorescence microscopy. (C) LNCaP cells were incubated with different concentrations of DHA, and apoptosis assay was analyzed by a Muse cell analyzer. (D) Quantification of apoptotic cells. Data are presented as mean ± SD, $n = 5$. $^{**}P < 0.01$ compared with control.

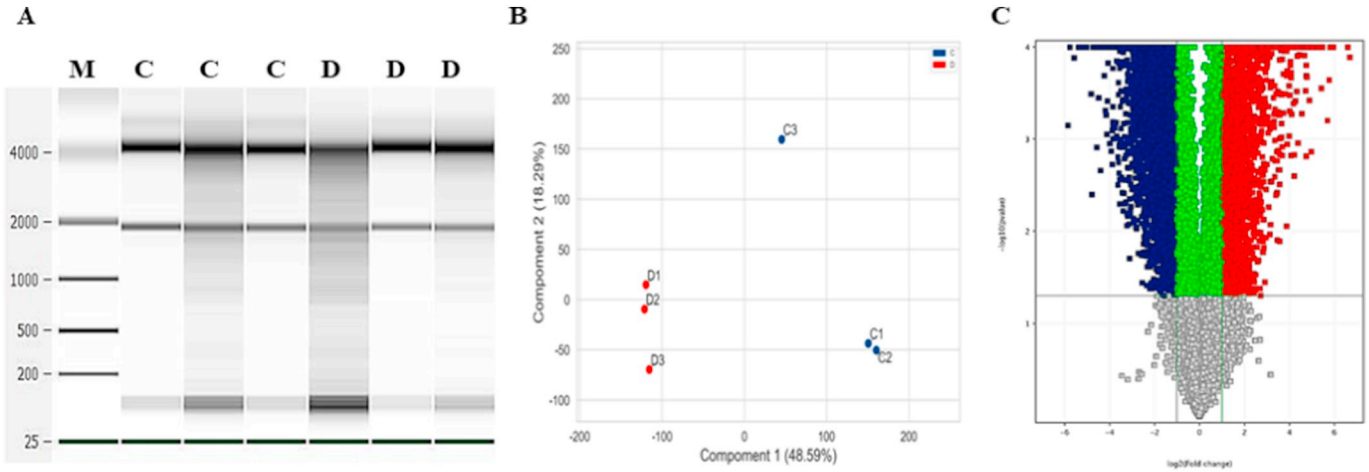

Fig. 2. Sample quality control and mRNA microarray analysis. (A) After treatment with DHA for 48 h, the total RNA was extracted to detect the integrity by formaldehyde agarose gel electrophoresis. M.DNA marker; C. Control group; D. DHA treated group. (B) PCA of **LNCaP** cells based on C untreated control and DHA treatment groups. (C) Volcano plots to determine DEGs of C *vs* D. The x-axis represents the log 2.0-fold changes (FC) of genes and the y-axis represents the $-\log^{10}$ of the *p-values* for the various condition pairs. Each dot represents a gene. The gray and the green points represent no statistically significant difference in gene expression. The red field represents the upregulated genes and the blue field represents the downregulated genes, which meet the selection threshold of $FC > 2.0$ and $p < 0.05$. (For interpretation of the references to colour in this figure legend, the reader is referred to the web version of this article.)

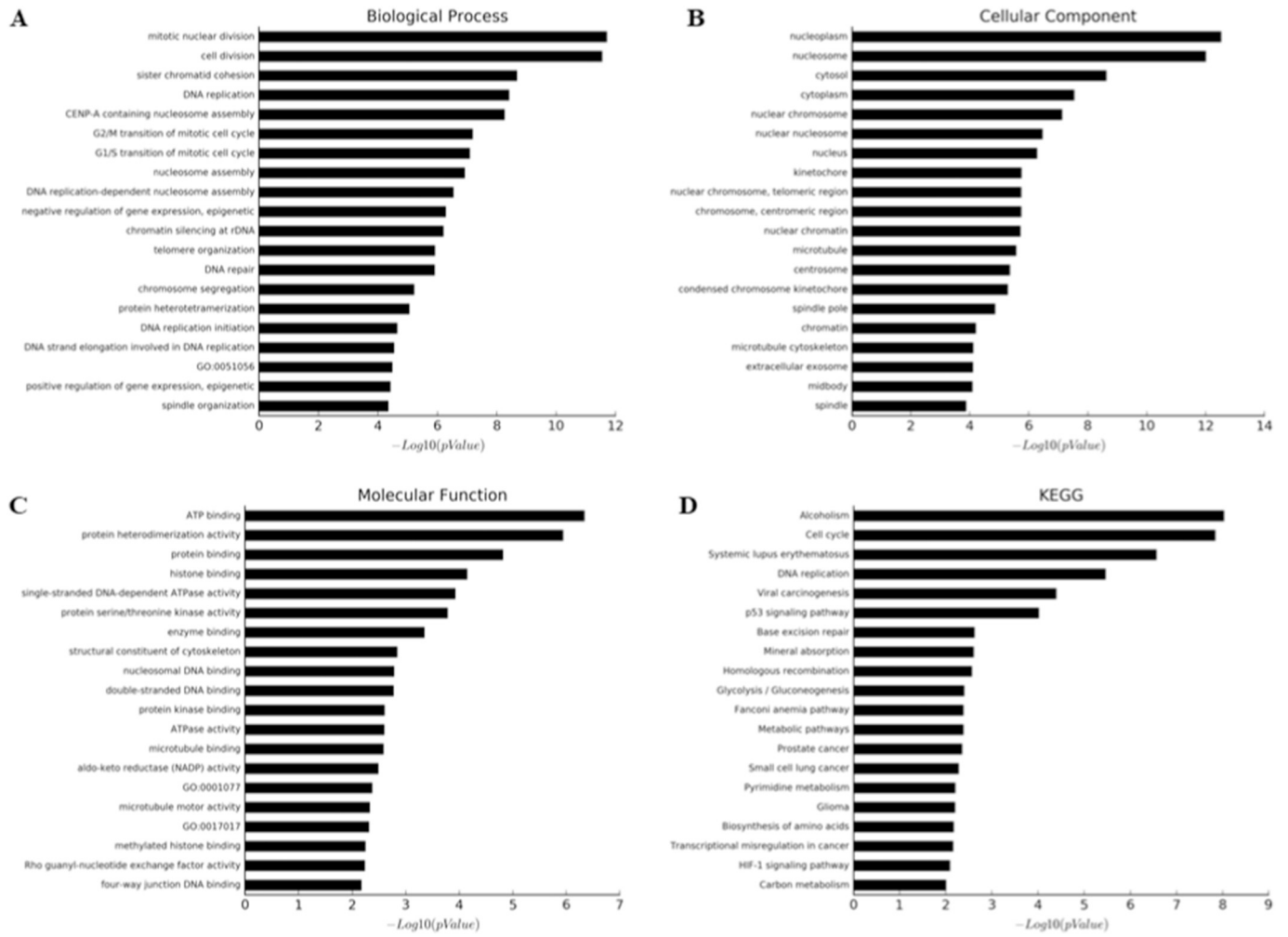

Fig. 3. GO and pathway analysis of DEGs in DHA-treated LNCaP cells. (A) Biochemical processes. (B) Cellular components. (C) Molecular function. (D) Percentage of DEGs in top 20 enriched pathways.

the stimulation of glycolytic enzymes, such as Glut, LDH, and PKM2. Consistent with the microarray results, Western blot indicated that DHA treatment decreased the expression of HIF-1α and expression rates of p-mTOR/mTOR and p-AKT/AKT (Fig. 8).

4. Discussion

In previous decades, remarkable progress has been achieved in therapeutic strategies for prostate cancer, one of the most malignant tumors with high relapse and mortality rates in men around the world [22]. In the current study, DHA intervention for prostate cancer LNCaP cells was performed to explore new therapeutic strategies. Using mRNA microarray expression profiling data, we found that regulating the metabolic pathway was involved in the process through which DHA inhibits the proliferation of LNCaP cells and aerobic glycolysis, which is crucial for the antitumor activity of DHA on prostate cancer.

DHA, the primary active product of ART and its derivatives, exhibits the strongest anticancer effect among these substances. Studies have shown that DHA has a slight effect on normal cells. Previous research has reported the anti-proliferation and metastasis of ART on prostate cancer and inducement of apoptosis [16,23]. Therefore, due to its minimal side effects, DHA is a likely candidate for use in prostate cancer treatment. In our study, DHA can significantly inhibit LNCaP cell proliferation in a dose-dependent manner *in vitro*. The apoptosis-detected results revealed that DHA-treated LNCaP cells demonstrate an apoptosis trend. However, the possible mechanism of DHA-induced LNCaP cell apoptosis should be investigated further.

RNA microarrays can provide snapshots of gene expressions across all of the genes in the genome. This method has been widely used in the systematic exploration of transcriptome information, including genetic and epigenetic factors and regulatory networks that cannot be reconstructed from protein-coding RNAs alone [24–26]. In the current studies, mRNA microarrays were adopted to analyze the gene expression in DHA-treated LNCaP cells to explore the possible mechanism. The mRNA microarray analysis results revealed that 3615 DEGs were involved in the process of DHA inhibiting the proliferation of LNCaP cells. Further analysis results showed that the DEGs can be attributed to ATP binding, protein binding, single-stranded DNA-dependent ATPase activity, and ATPase activity. The pathways of cell cycle, DNA replication, p53 signaling, glycolysis/gluconeogenesis, metabolism, pyrimidine metabolism, HIF-1 signaling, and biosynthesis of amino acids showed the highest correlation with DHA inhibiting the proliferation of LNCaP cells. p53 activation is induced by a number of stress signals, including DNA damage, oxidative stress, and activated oncogenes [27]. This condition results in three major outputs: cell cycle arrest, cellular senescence, or apoptosis. Glycolysis, the process of converting glucose into pyruvate and generating ATP, is a central pathway that produces important precursor metabolites [28]. Gluconeogenesis is a synthesis pathway of glucose from non-carbohydrate precursors [29]. It is essentially a reversal of glycolysis with minor variations of alternative paths. HIF-1 can induce the expression of GLUT-1, LDHA, PFKP, aldolase A, enolase 1, and phosphoglycerate kinase 1 [30,31]. In conclusion,

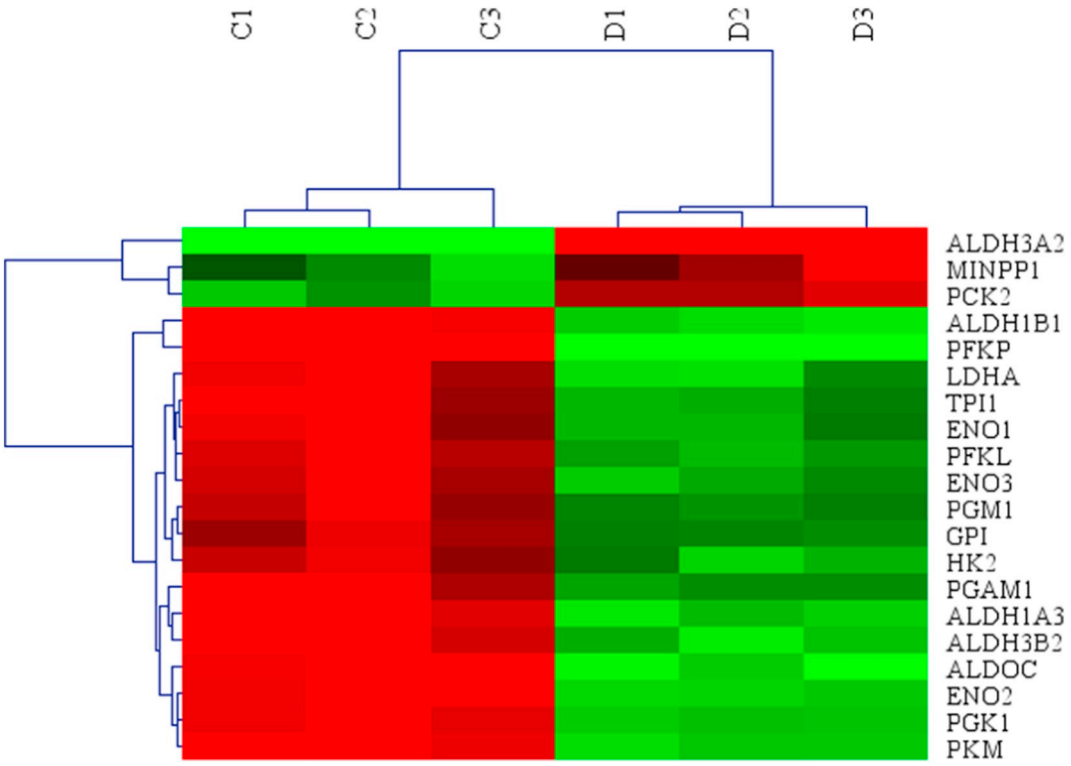

Fig. 4. Heat map displaying DEGs induced by DHA treatment in glycolysis/gluconeogenesis pathway. Red and green colors indicate high and low expressions, respectively. (For interpretation of the references to colour in this figure legend, the reader is referred to the web version of this article.)

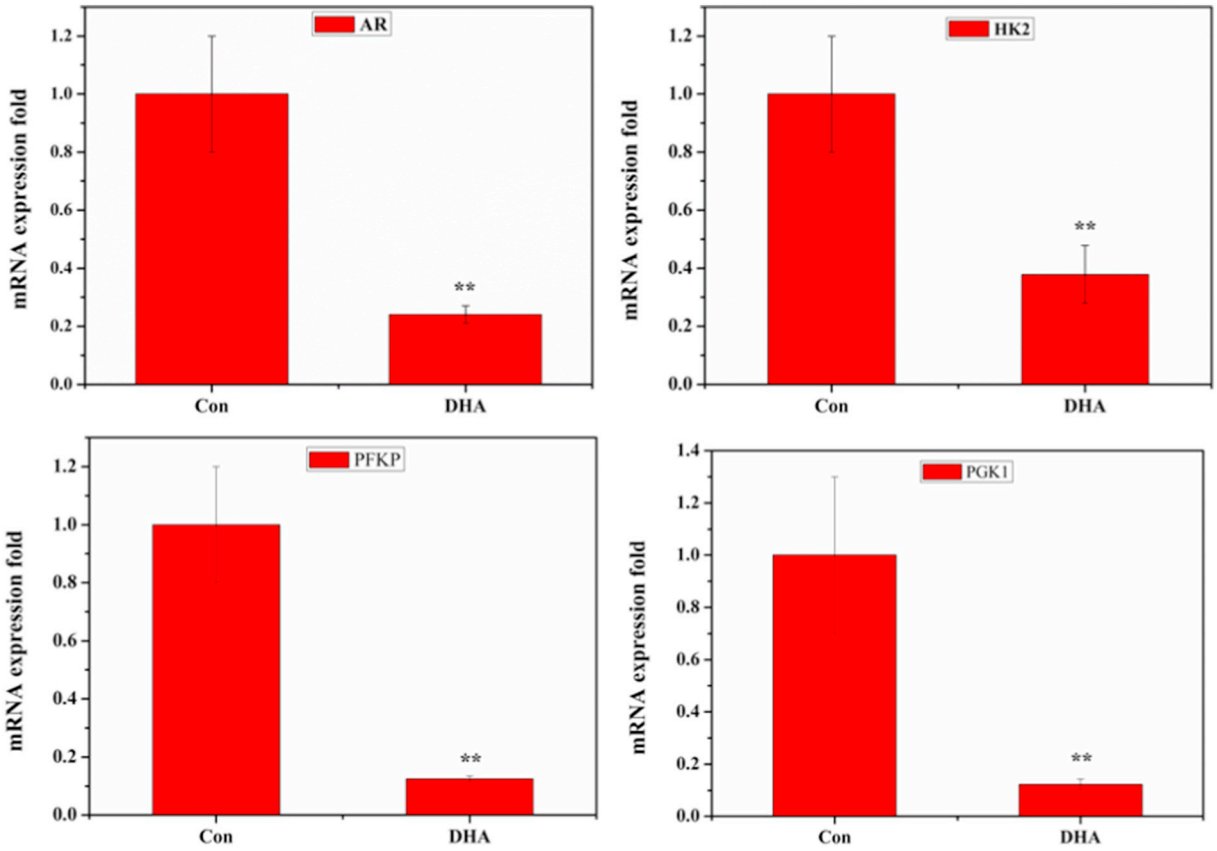

Fig. 5. mRNA levels of four selected genes in LNCaP cells as detected by qRT-PCR.

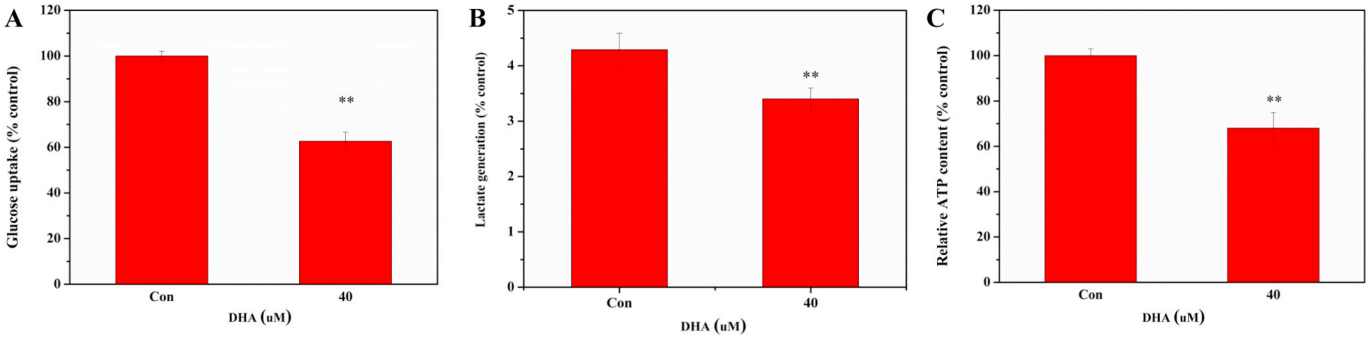

Fig. 6. DHA suppress glycolysis level in LNCaP cells. (A) After LNCaP cells were treated with 40 uM DHA for 48 h. Glucose content in the culture media was immediately tested, and glucose uptake was calculated. (B) Lactate content was detected. (C) ATP content was detected through bioluminescence assay. Data are presented as mean ± SD, n = 5. $^{**}P < 0.01$ compared with control.

glycolysis inhibition was involved in the process through which DHA inhibited the proliferation of LNCaP cells. The transcriptome data may serve as a starting point for further mechanism analysis.

The metabolic switch toward aerobic glycolysis has been reported as a feature called Warburg effect [32,33]. This effect is a metabolic reprogramming process used by cancer cells to support their high-energy requirements and high rates of macromolecular synthesis. Several glycolytic enzymes, including HK2, PFKP, PKM2, and LDH, control the Warburg effect. GLUT-1 is significantly correlated with the Warburg effect, which can facilitate the transport of glucose across the plasma membrane of the cell where it is utilized for cellular metabolism [30,34,35]. To further confirm the effect of DHA on prostate cancer glycolysis, we applied Western blot to detect the expression of glycolytic regulator proteins in LNCaP cells. The results showed that DHA treatment can decrease the expressions of GLUT1, HK2, PFKP, PKM2, and LDH. The preceding results show that DHA can inhibit glycolysis in LNCaP cells.

An increased rate of glucose metabolism is associated with the overactivation of the PI3K/Akt pathway [36]. The activation of this pathway stimulates HIF-1α, which induces stimulation of glycolytic enzymes such as Glut, LDH, and PKM2 [35,37]. In the current study, we found that DHA treatment can reduce the expression of HIF-1α, p-mTOR/mTOR, and p-AKT/AKT. We surmised that overall, DHA modulates HIF-1α expression through the PI3K/AKT pathway to inhibit the glycolysis in LNCaP cells.

5. Conclusions

The data from this study indicate that DHA treatment can depress LNCaP cell proliferation and induce cell apoptosis. The possible mechanism may be related to a decrease of glycolysis by inhibiting the intracellular PI3K/AKT pathway, which is associated with HIF-1α. Our study suggests that DHA is a potential therapeutic agent for the treatment of prostate cancer in the future.

Supplementary data to this article can be found online at https://doi.org/10.1016/j.lfs.2019.116730.

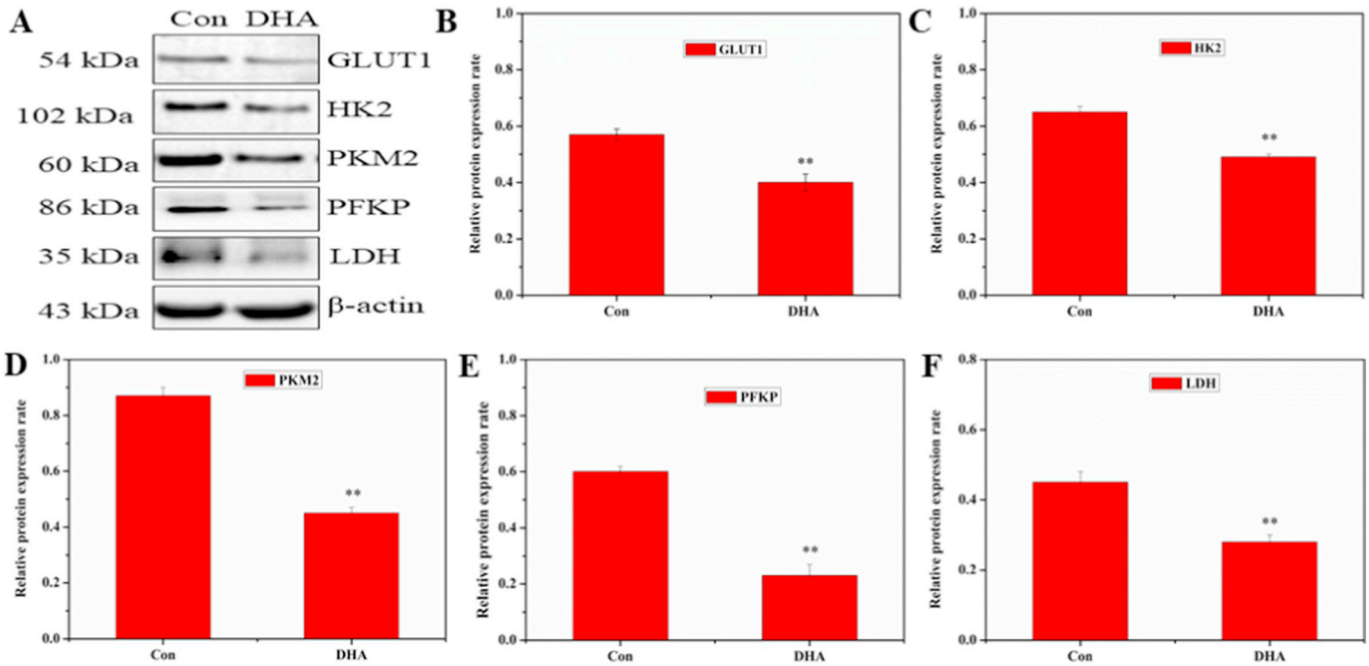

Fig. 7. Effect of DHA on expression of glycolytic regulatory proteins. (A) LNCaP cells were treated with 40 μM DHA for 48 h. Protein expression was analyzed using Western blot and quantified in relation to β-actin. (B–F) Densitometric values were normalized by β-actin and expressed as mean ± SD, $n = 3$. $^{**}P < 0.01$ compared with control.

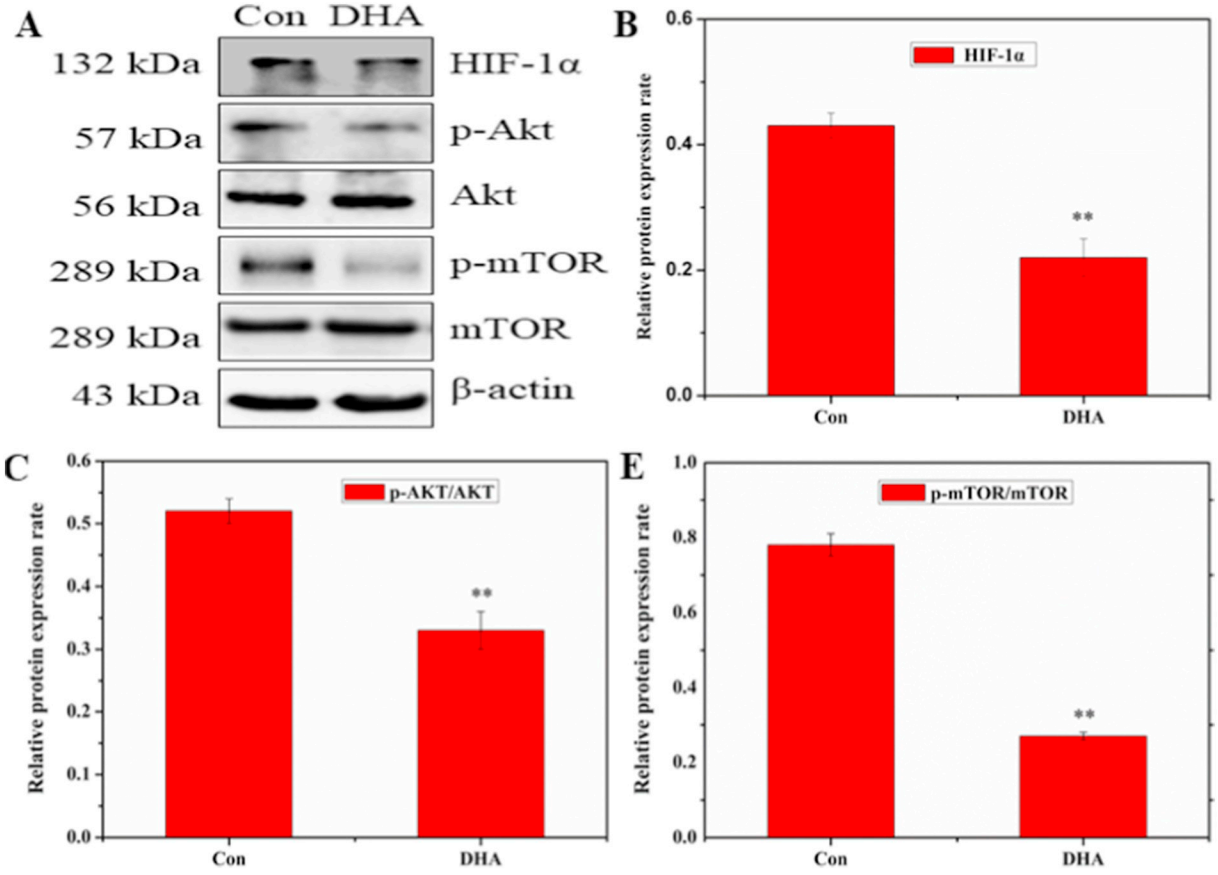

Fig. 8. Effect of DHA on expression of HIF-1α and PI3K/AKT pathway relative proteins. (A) LNCaP cells were treated with 40 μM DHA for 48 h. Protein expression was analyzed using Western blot and quantified in relation to β-actin. (B–F) Densitometric values were normalized by β-actin and expressed as mean ± SD, n = 3. $^{**}P < 0.01$ compared with control.

Abbreviations

Akt	Protein kinase B
DMEM	Dulbecco's Modified Eagle's Medium
DHA	Dihydroartemisinin
DMSO	Dimethyl sulfoxide
DEGS	Differentially expressed genes
FBS	Fetal bovine serum
GO	Gene ontology
Glut 1	Glucose transporter 1
HIF-1α	Hypoxia-inducible factor-1α
KEGG	Kyoto Encyclopedia of Genes and Genomes
PI3K	Phosphatidylinositol-4,5-bisphosphate 3-kinase
PCA	Principal Component analysis
qRT-PCR	Quantitative reverse transcription PCR

Funding

This work was supported by National Natural Science Foundation of China (31572262, C040301), Project Agreement for Science & Technology Development, Jilin Province (No. 20170414022GH, No. 20190201148JC and No. 20160101198JC), Excellent Youth Talents Training programs of Jilin City (No. 20156428) and the Jilin Provincial Health and Family Planning Commission (2015Q041) and Jilin Collaborative Innovation Center for Antibody Engineering (20180623045TC).

Declaration of competing interest

The authors declare that there is no conflict of interest.

References

[1] K.J. Harrington, C. Spitzwg, A.R. Bateman, et al., Gene therapy for prostate cancer: current status and future prospects, J. Urol. 166 (4) (2001) 1220–1233, https://doi.org/10.1016/S0022-5347(05)65742-4.
[2] C.H. Pernar, E.M. Ebot, K.M. Wilson, et al., The epidemiology of prostate cancer, Cold Spring Harbor Perspect. Med. a030361 (2018), https://doi.org/10.1016/S0094-0143 (02)00181-7.
[3] E.M. Sebesta, C.B. Anderson, The surgical management of prostate cancer, Semin. Oncol. 44 (5) (2018) 347–357, https://doi.org/10.1053/j.seminoncol.2018.01.003.
[4] M. Bolla, L. Collette, D. Gonzalez, et al., Long term results of immediate adjuvant hormonal therapy with goserelin in patients with locally advanced prostate cancer treated with radiotherapy—a phase III EORTC study, Eur. J. Cancer 35 (3) (1999) 147, https://doi.org/10.1016/S0360-3016(99)90023-8.
[5] H. Copp, E.A. Bissonette, T. Dan, Tumor control outcomes of patients treated with trimodality therapy for locally advanced prostate cancer, Urology 65 (6) (2005) 1146–1151, https://doi.org/10.1016/j.urology.2004.12.014.
[6] L. Souhami, K. Bae, M. Pilepich, et al., Impact of the duration of adjuvant hormonal therapy in patients with locally advanced prostate cancer treated with radiotherapy: a secondary analysis of RTOG 85-31, J. Clin. Oncol. 27 (13) (2009) 2137–2143, https://doi.org/10.1200/JCO.2008.17.4052.
[7] J.L. Tang, B.Y. Liu, K.W. Ma, Traditional Chinese medicine, Lancet 372 (9654) (2008) 1938–1940, https://doi.org/10.1016/S0140-6736(08)61354-9.
[8] A.M. Dondorp, R.M. Fairhurst, Artemisinin resistance in Plasmodium falciparum malaria, N. Engl. J. Med. 361 (18) (2009) 455–467, https://doi.org/10.1056/NEJMc091737.
[9] U.S. Neill, From branch to bedside: Youyou Tu is awarded the 2011 Lasker~DeBakey Clinical Medical Research Award for discovering artemisinin as a treatment for malaria, J. Clin. Invest. 121 (10) (2011) 3768–3773, https://doi.org/10.1172/JCI60887.
[10] N.C. Danbolt, Glutamate uptake, Prog. Neurobiol. 65 (1) (2001) 1–105, https://doi.org/10.1016/s0301-0082(00)00067-8.
[11] C. Schultz, A. Link, M. Leost, Paullones, a series of cyclin-dependent kinase inhibitors: synthesis, evaluation of CDK1/cyclin B inhibition, and in vitro antitumor activity, J. Med. Chem. 42 (15) (1999) 2909–2919, https://doi.org/10.1021/jm9900570.
[12] C.Z. Zhang, H. Zhang, J. Yun, et al., Dihydroartemisinin exhibits antitumor activity toward hepatocellular carcinoma in vitro and in vivo, Biochem. Pharmacol. 83 (9)

(2012) 1278–1289, https://doi.org/10.1016/j.bcp.2012.02.002.
[13] L. Cui, Z.L. Wang, J. Miao, M. Miao, R. Chandra, H.Y. Jiang, X.Z. Su, L.W. Cui, Mechanisms of in vitro resistance to dihydroartemisinin in plasmodium falciparum, Mol. Microbiol. 86 (1) (2012) 111–128, https://doi.org/10.1111/j.1365-2958.2012.08180.x.
[14] V.A. Pashynska, H.V.D. Heuvel, M. Claeys, M.V. Kosevich, Characterization of noncovalent complexes of antimalarial agents of the artemisinin-type and Fe(III)-heme by electrospray mass spectrometry and collisional activation tandem mass spectrometry, J. Am. Soc. Mass Spectrom. 15 (8) (2004) 1181–1190, https://doi.org/10.1016/j.jasms.2004.04.030.
[15] H.R. Christofk, M.G. Vander Heiden, M.H. Harris, et al., The M2 splice isoform of pyruvate kinase is important for cancer metabolism and tumour growth, Nature 452 (7184) (2008) 230–233, https://doi.org/10.1038/nature06734.
[16] P.P. Hsu, D.M. Sabatini, Cancer cell metabolism: Warburg and beyond, Cell 134 (5) (2008) 703–707, https://doi.org/10.1016/j.cell.2008.08.021.
[17] S. Pavlides, A. Tsirigos, I. Vera, et al., Transcriptional evidence for the “reverse Warburg effect” in human breast cancer tumor stroma and metastasis: similarities with oxidative stress, inflammation, Alzheimer’s disease, and “neuron-glia metabolic coupling”, Aging 2 (4) (2010) 185–199, https://doi.org/10.18632/aging.100134.
[18] F. Sotgia, D. Whitakermenezes, U.E. Martinezoutschoorn, et al., Mitochondrial metabolism in cancer metastasis: visualizing tumor cell mitochondria and the "reverse Warburg effect" in positive lymph node tissue, Cell Cycle 11 (7) (2012) 1445–1454, https://doi.org/10.4161/cc.19841.
[19] E. Lavallée, M. Bergeron, F.A. Buteau, et al., Increased prostate cancer glucose metabolism detected by 18F-fluorodeoxyglucose positron emission tomography/computed tomography in localised Gleason 8–10 prostate cancers identifies very high-risk patients for early recurrence and resistance to castration, European Urology Focus (2018), https://doi.org/10.1016/j.euf. 2018.03.008 S2405456918300865.
[20] R.K. Ross, G.A. Coetzee, C.L. Pearce, et al., Androgen metabolism and prostate Cancer: establishing a model of genetic susceptibility, Eur.Urol. 35 (5–6) (1999) 355–361, https://doi.org/10.1016/j.canep.2012.04.002.
[21] K.J. Livak, T.D. Schmittgen, Analysis of relative gene expression data using real-time quantitative PCR and the 2(−Delta Delta C(T)) method, Methods 25 (4) (2001) 402–408, https://doi.org/10.1006/meth.2001.
[22] P.R. Twentyman, M. Luscombe, A study of some variables in a tetrazolium dye (MTT) based assay for cell growth and chemosensitivity, Br. J. Cancer 56 (3) (1987) 279–285, https://doi.org/10.1038/bjc.1987.190.
[23] A. Dondorp, F. Nosten, K. Stepniewska, et al., Artesunate versus quinine for treatment of severe falciparum malaria: a randomised trial, Lancet 366 (9487) (2005) 717–725, https://doi.org/10.1016/S0140-6736(05)67176-0.
[24] X. Fu, N. Fu, S. Guo, et al., Estimating accuracy of RNA-Seq and microarrays with proteomics, BMC Genomics 10 (1) (2009) 161, https://doi.org/10.1186/1471-2164-10-161.
[25] C.G. Liu, G.A. Calin, S. Volinia, et al., MicroRNA expression profiling using microarrays, Nat. Protoc. 3 (4) (2008) 563–578, https://doi.org/10.1038/nprot.2008.14.
[26] J.Q. Yin, R.C. Zhao, K.V. Morris, Profiling microRNA expression with microarrays, Trends Biotechnol. 26 (2) (2008) 70–76, https://doi.org/10.1016/j.tibtech.2007.11.007.
[27] A. Hirao, Y.Y. Kong, S. Matsuoka, et al., DNA damage-induced activation of p53 by the checkpoint kinase Chk2, Science 287 (5459) (2000) 1824–1827, https://doi.org/10.1126/science.287.5459.1824.
[28] S. Ganapathy-Kanniappan, J.F. Geschwind, Tumor glycolysis as a target for cancer therapy: progress and prospects, Mol. Cancer 12 (1) (2013) 152, https://doi.org/10.1126/science.287.5459.1824.
[29] T.Y. Liu, C.X. Shi, R. Gao, et al., Irisin inhibits hepatic gluconeogenesis and increases glycogen synthesis via the PI3K/Akt pathway in type 2 diabetic mice and hepatocytes, Clin. Sci. 129 (10) (2015) 839–850, https://doi.org/10.1042/cs20150009.
[30] F.L. Byrne, I.K. Poon, S.C. Modesitt, et al., Metabolic vulnerabilities in endometrial cancer, Cancer Res. 74 (20) (2014) 5832, https://doi.org/10.1158/0008-5472.CAN-14-0254.
[31] H. Sylvia, A. Claudio, D. Jürgen, et al., GLUT1 expression patterns in different Hodgkin lymphoma subtypes and progressively transformed germinal centers, BMC Cancer 12 (1) (2012) 586, https://doi.org/10.1186/1471-2407-12-586.
[32] L. Sun, C. Suo, S.T. Li, et al., Metabolic reprogramming for cancer cells and their microenvironment: beyond the Warburg effect, Biochim. Biophys. Acta, Rev. Cancer 1870 (1) (2018) 51–66, https://doi.org/10.1016/j.bbcan.2018.06.005 (S0304419X18300350).
[33] A.G. Vlassenko, B.A. Gordon, M.S. Goyal, et al., Aerobic glycolysis and tau deposition in preclinical Alzheimer disease, Neurobiol. Aging (2018), https://doi.org/10.1016/j.neurobiolaging.2018.03.014 67S0197458018300927.
[34] S.Y. Kim, S.J. Sohn, A.J. Won, et al., Identification of noninvasive biomarkers for nephrotoxicity using HK-2 human kidney epithelial cells, Toxicol. Sci. 140 (2) (2014) 247–258, https://doi.org/10.1093/toxsci/kfu096.
[35] H. Wang, C. Zhang, L. Xu, et al., Bufalin suppresses hepatocellular carcinoma invasion and metastasis by targeting HIF-1α via the PI3K/AKT/mTOR pathway, Oncotarget 7 (15) (2016) 20193–20208, https://doi.org/10.18632/oncotarget.7935.
[36] B.T. Hennessy, D.L. Smith, P.T. Ram, et al., Exploiting the PI3K/AKT pathway for cancer drug discovery, Nat. Rev. Drug Discov. 4 (12) (2005) 988–1004, https://doi.org/10.1038/nrd1902.
[37] Z. Ye, Q. Guo, P. Xia, et al., Sevoflurane postconditioning involves an up-regulation of HIF-1α and HO-1 expression via PI3K/Akt pathway in a rat model of focal cerebral ischemia, Brain Res. 1463 (2012) 63–74, https://doi.org/10.1016/j.brainres.2012.04.050.